

# Photovoltaic Conversion Enhancement of a Carbon Quantum Dots/p-Type CuAlO<sub>2</sub>/n-Type ZnO Photoelectric Device

Jiaqi Pan,<sup>†,‡</sup> Yingzhuo Sheng,<sup>†,‡</sup> Jingxiang Zhang,<sup>‡</sup> Peng Huang,<sup>†,‡</sup> Xin Zhang,<sup>\*,‡,§</sup> and Boxue Feng<sup>\*,†,‡</sup>

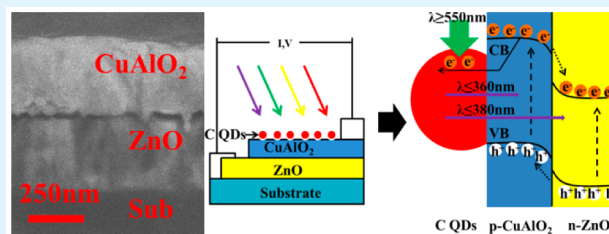
<sup>†</sup>Key Laboratory for Magnetism and Magnetic Materials of Ministry of Education and <sup>‡</sup>School of Physical Science and Technology, Lanzhou University, Lanzhou 730000, P. R. China

<sup>§</sup>College of Science, Xi'an University of Science and Technology, Xi'an 710000, P. R. China

## Supporting Information

**ABSTRACT:** Carbon quantum dots (C QDs)/p-type CuAlO<sub>2</sub>/n-type ZnO photoelectric bilayer film composites were prepared by a simple route, through which ZnO films were sputtered on crystal quartz substrates and CuAlO<sub>2</sub> films were prepared by sol-gel on ZnO films and then these bilayer films were composited with C QDs on their surface. The characterization results indicated that C QDs were well combined with the surface of the CuAlO<sub>2</sub> films. The photovoltage and photocurrent of these bilayer film composites were investigated under illumination and darkness switching, which demonstrated to be significantly enhanced compared with those of the CuAlO<sub>2</sub>/ZnO bilayer films. Through analysis, this enhancement of the photoconductivity was mainly attributed to C QDs with unique up-converted photoluminescence behavior.

**KEYWORDS:** carbon quantum dots, p-n junction, transmittance, up-converted photoluminescence, photoelectric



## 1. INTRODUCTION

In the past decade, with the rapid increase of global energy demand, how to exploit and utilize the solar energy has become a research focus. Of varied ways, solar cells, with their promising applications in utilizing solar energy, have been one of the most popular ways to convert solar energy.<sup>1–3</sup> Especially, a transparent p–n junction-type device,<sup>4,5</sup> with its high transmittance and chemical stability, has grabbed much attention for being able to be applied in functional windows. As is known, the foundation of this type of device is a transparent conducting oxide (TCO). Up to now, lots of n-type TCOs have been reported,<sup>6,7</sup> such as ZnO, In<sub>2</sub>O<sub>3</sub>, etc., but the lack of p-type TCOs restricted the development of a transparent photoelectric device. Although GaN, etc., have been prepared as p-type materials,<sup>8</sup> because of their cost, they can hardly be applied in mass industrial manufacturing. For all of these reasons, finding an intrinsic p-type material has been an urgent issue. Calculations indicate that AMO<sub>2</sub>-type delafossite may be a potential choice, particularly CuAlO<sub>2</sub>, with its p-type conductivity, chemical stability, and ruggedness attracting much attention since the CuAlO<sub>2</sub> films were first reported in 1997.<sup>9–12</sup> Lots of researchers have tried to introduce this p-type TCO into transparent solar cells; for instance, Kim et al. prepared a p–n junction thin-film diode,<sup>13</sup> and Banerjee et al. prepared a p-type CuAlO<sub>2+x</sub>/n-type Zn<sub>1-x</sub>Al<sub>x</sub>O junction transparent diode.<sup>14</sup> However, it is a pity that there is still a serious problem: the efficiency of solar energy utilization. As is known, most of the Earth's surface sunlight is visible light, but in order to maintain excellent transmittance, most of the p–n-type devices are composed of wide-band-gap TCOs, which

cannot economize solar energy. So, we hope to develop a device with both high transmittance and efficient utilization for solar energy.

On the other hand, carbon materials, with their environmentally friendly, nontoxic degradable, and low-cost features, have been a new direction in current research. Lots of studies on different carbon forms such as carbon nanotubes, carbon nanowires, graphene, etc., have been reported.<sup>15,16</sup> Among them, carbon quantum dots (C QDs), with their excellent fluorescence and up-conversion properties, have been widely applied in cell imaging,<sup>17</sup> visible-light photocatalysis, etc. For instance, Liu et al. prepared C QDs/TiO<sub>2</sub> nanosheet composites for visible-light photocatalytic activity,<sup>18</sup> Luo et al. used C QDs for photovoltaic devices and self-driven photodetectors,<sup>19</sup> and Xu et al. prepared a graphene/TiO<sub>2</sub> composite to improve visible-light photocatalytic activity.<sup>20</sup> Unquestionably, these properties of C QDs may provide us with a new method to solve the problem mentioned above. We attempt to introduce the C QDs into the p–n junction to convert a part of the visible light to high-frequency near-ultraviolet light, which may maintain both the high transmittance and efficient utilization for solar energy. What is more, in our design, we cover the wider-band-gap semiconductor CuAlO<sub>2</sub> on ZnO (C QDs/p-type CuAlO<sub>2</sub>/n-type ZnO), which could take advantage of the solar energy more efficiently.

Received: November 21, 2014

Accepted: March 30, 2015

Published: March 30, 2015

In this work, we prepared a C QDs/p-type  $\text{CuAlO}_2$ /n-type ZnO device via a simple route of radio-frequency (RF) magnetron sputtering and sol-gel. The results show that the devices possess excellent photosensitivity and high transmittance. Furthermore, the mechanism of enhancement of photovoltaic conversion was studied.

## 2. EXPERIMENTAL SECTION

**2.1. Preparation. Fabrication of ZnO Films.** ZnO films were prepared by RF magnetron sputtering using a ZnO target (5 cm diameter). A crystalline quartz plate was used as the substrate. The back vacuum was  $6 \times 10^{-3}$  Pa, and the sputtering power was 45 W. The work pressure and deposition time were 0.5 Pa and 1.5 h, respectively. The substrate was grounded. The sputtering gas (45 SCCM) was argon. After deposition, all of the as-prepared films were annealed at 450 °C for 2 h in air.

**Fabrication of  $\text{CuAlO}_2$  Films.** In detail, 5 g of polyethyleneimine was first dissolved in 70 mL of water and stirred for 3 h, followed by the addition of 2.46 g of  $\text{Cu}(\text{NO}_3)_2 \cdot 3\text{H}_2\text{O}$  and 3.75 g of  $\text{Al}(\text{NO}_3)_3 \cdot 9\text{H}_2\text{O}$  to the solution. Then the whole mixture was again stirred at room temperature for 3 h to obtain a well-mixed precursor solution. The precursor with the desired stoichiometry ratio was spun-coated onto the as-prepared ZnO films at 2500 rpm for 30 s. Finally, the bilayer films were heated at 1050 °C for 75 min in air.<sup>21</sup>

**Fabrication of C QDs.** First, 0.75 g of sucrose was dispersed into 30 mL of deionized water under magnetic stirring for 30 min. Then, the mixture was transferred to a 40 mL Teflon-lined stainless steel autoclave and heated at 180 °C for 5 h. After completion of the reaction, the autoclave was cooled to room temperature naturally. The solution was filtered to separate the deposit, and the brown filtrate was then centrifuged at high speed to obtain high-quality C QDs (Figure S1 in the Supporting Information, SI).

**Fabrication of a C QDs/p-Type  $\text{CuAlO}_2$ /n-Type ZnO Photoelectric Device.** A total of 100 mg of C QDs was obtained and dissolved in 100 mL of water, and the concentration of the C QDs solution was 1 mg/mL. C QDs/ $\text{CuAlO}_2$  films were synthesized by a simple route in which 0.1 mL of a C QDs solution (1 mg/mL) was dropped onto the surface of a  $1 \times 1 \text{ cm}^2$   $\text{CuAlO}_2$  film and dried at 80 °C for 8 h. C QDs/ $\text{CuAlO}_2$  films prepared by changing the concentration of the C QDs solution of 0, 1.0, 2.0, and 3.0 mg/mL were labeled as C/F 0, C/F 1, C/F 2, and C/F 3, respectively.

**2.2. Characterization.** The morphologies and crystallography of the samples were characterized by field-emission scanning electron microscopy (SEM; Hitachi S-4800) and high-resolution transmission electron microscopy (HRTEM; Tecnai-G2 F30). The structures of the samples were characterized by X-ray diffraction (XRD; Rigaku D/MAX-2400). X-ray photoelectron spectroscopy (XPS) data were measured by an ESCALAB-250 spectrometer. The optical properties were measured with a TU-1901 dual-beam UV-vis spectrophotometer using a deuterium lamp. The photoluminescence (PL) spectra were measured at room temperature with a FLs920 steady state/transient state spectro sort with a xenon lamp in a water solution, and Fourier transform infrared (FT-IR) spectra were measured by a Thermo Nicolet Nexus FT-IR model 670 spectrometer with the KBr pellet technique. The electrical properties such as the dark and illuminated currents were measured by an electrochemical workstation. The sunlight was calibrated by a xenon lamp, and the light intensity amounted to 100  $\text{mW}/\text{cm}^2$ .

## 3. RESULTS AND DISCUSSION

Structure characterization of the C QDs/p-type  $\text{CuAlO}_2$ /n-type ZnO films is shown in Figure 1. Figure 1a is the XRD spectra of the samples on quartz substrates. As revealed, all of the samples exhibit the same characteristic diffraction peaks of delafossite  $\text{CuAlO}_2$  (PDF 21-0276) and ZnO (PDF 36-1451). No obvious characteristic diffraction peak of carbon is detected, which is attributed to the small amounts and low crystallinity of C QDs. Figure 1b is the SEM image of the sample. As can be seen, it is

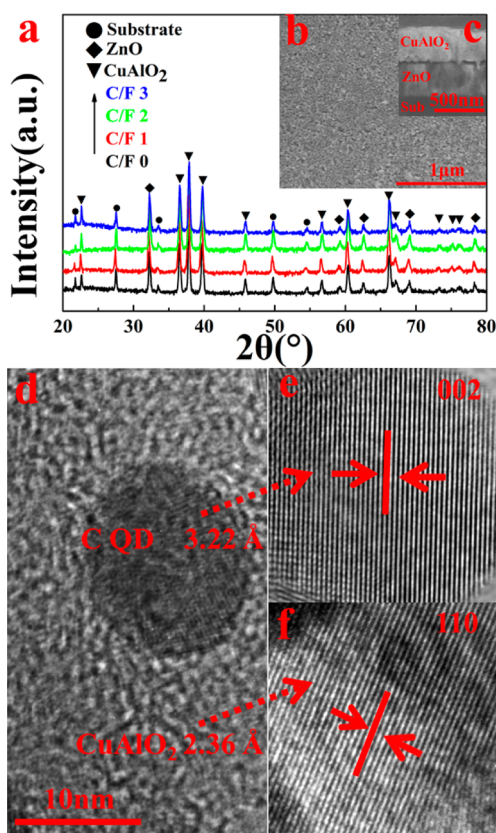


**Figure 1.** Structure of as-prepared C QDs/p-type  $\text{CuAlO}_2$ /n-type ZnO film composites. (a) XRD patterns of C QDs/ $\text{CuAlO}_2$ /ZnO film composites with different amounts of C QDs. (b) SEM images of C QDs/ $\text{CuAlO}_2$ /ZnO film composites. (c) Sectional drawing of the sample. (d) TEM images of C QDs/ $\text{CuAlO}_2$ /ZnO film composites. (e and f) HRTEM images of the C QD and  $\text{CuAlO}_2$  film.

obvious that the sample is homogeneous, smooth, and continuous. Figure 1c is the sectional drawing of the sample. As can be seen, the sample is composed of  $\text{CuAlO}_2$  and ZnO. Considering the limited resolution and size, the C QDs could not be seen. However, from the TEM images, as shown in Figure 1d, it can be observed that the C QD is attached to the surfaces of the  $\text{CuAlO}_2$  film. Parts e and f of Figure 1 show the HRTEM images of the C QD and  $\text{CuAlO}_2$ . The lattice spacing of 0.238 nm corresponds to the (110) planes of  $\text{CuAlO}_2$ , and the lattice spacing of 0.320 is in good agreement with the (002) plane of graphitic carbon.

Figure 2 shows the FT-IR spectra. The peaks at 3430 and 1630  $\text{cm}^{-1}$  appearing in p-type  $\text{CuAlO}_2$ /n-type ZnO and C QDs/p-type  $\text{CuAlO}_2$ /n-type ZnO films are attributed to vibrations of water absorbed onto the surface. The new peak at 1380  $\text{cm}^{-1}$  of the epoxy C–O stretching vibration appearing in C QDs/ $\text{CuAlO}_2$  films can be explained by the successful interactions between  $\text{CuAlO}_2$  films and C QDs.<sup>22,23</sup>

Furthermore, XPS was carried out to investigate the components and surface properties of the C QDs/p-type  $\text{CuAlO}_2$ /n-type ZnO films. As shown in Figure 3a, the main peak at 284.6 eV is attributed to the C–C bond with  $\text{sp}^2$  orbital. The peaks at 286.0 and 288.3 eV are assigned to the C–O and C=O bonds, respectively. What is more, no peak of the Cu–C and Al–C bonds is found in Figure 3a, which indicates that C QDs do not exist as dopants in composites. In Figure 3b, the peaks at 529.6, 530.1, 530.8, and 532.0 eV are ascribed to Al–

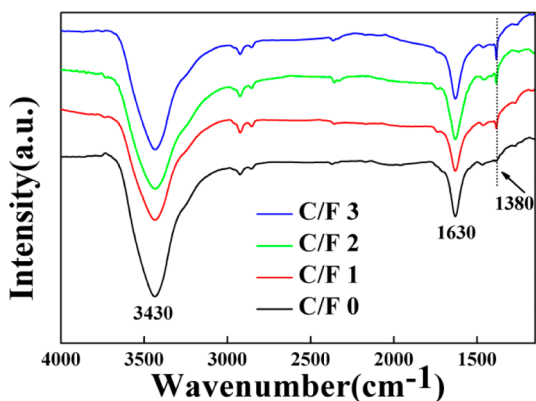


Figure 2. FT-IR spectra of C QDs/p-type  $\text{CuAlO}_2$ /n-type ZnO film composites.

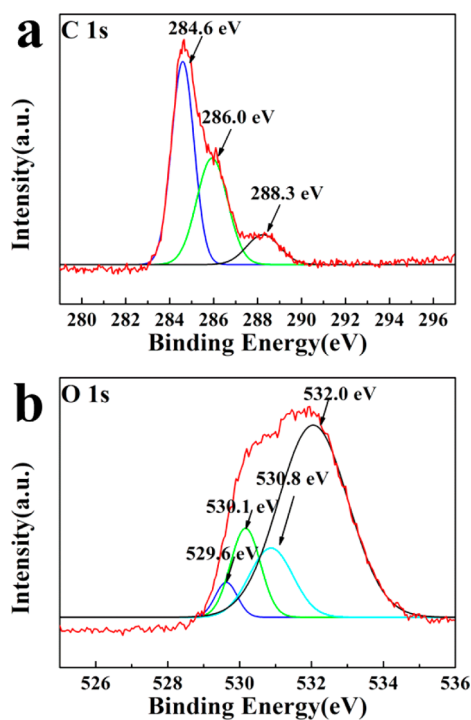


Figure 3. XPS spectra of C QDs/p-type  $\text{CuAlO}_2$ /n-type ZnO film composites: (a) C 1s; (b) O 1s.

O, Cu–O, C=O, and C–OH. Both parts a and b of Figure 3 indicate the existence of C–O bonds in C QDs/ $\text{CuAlO}_2$  films.

The optical transmittance ( $T$ ) spectra of C QDs/p-type  $\text{CuAlO}_2$ /n-type ZnO bilayer film composites with different C QD concentrations are fitted in Figure 4. The bilayer film thickness is of around 350 nm (each one) as measured by cross-sectional SEM, which is shown in Figure 1c. The spectra depict that the bilayer films have a highly visible transmittance of around  $\sim 50\%$  in average, which may meet the demand of window materials. Moreover, it can be seen that the transmittance decreased slightly with increasing C QD concentration, which indicates that the visible light is absorbed by additional C QDs. In spite of this, it barely affects its application. What is more, there is a sharp decrease in 380 nm for all samples, which is from the band gap of ZnO. As desired, the high transmittance can help these bilayer film composites to be applied to the transparent devices, and at the same time, the increasing visible-light utilization rate may increase the number

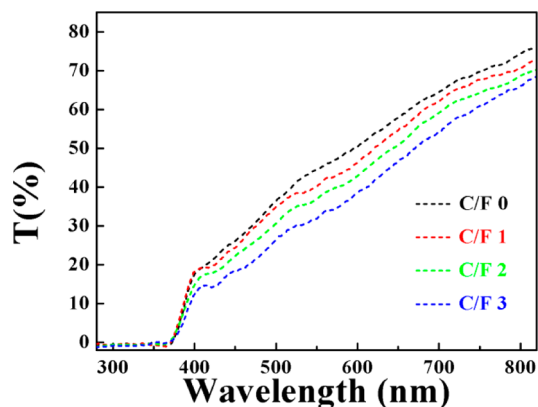


Figure 4. Optical transmittance ( $T$ ) spectra of C QDs/p-type  $\text{CuAlO}_2$ /n-type ZnO film composites with different amounts of C QDs.

of photogenerated carriers to improve the photocurrent. The similar curves indicate that the structures of the films were stable after C QDs were composited, which is helpful in explaining the influence from C QDs.<sup>21</sup>

In this work, we expect that the device could be used in the field of civil application, so all of the measurements were under simulated sunlight. All of the bilayer film devices exhibit photovoltaic behavior with an open-circuit voltage of  $\sim 220$  mV, which corresponds to previous reports and is available for application in photoelectric devices.<sup>24</sup>

Further, the photoelectric properties are shown in Figure 5. The evolution of the photoelectricity was measured at room

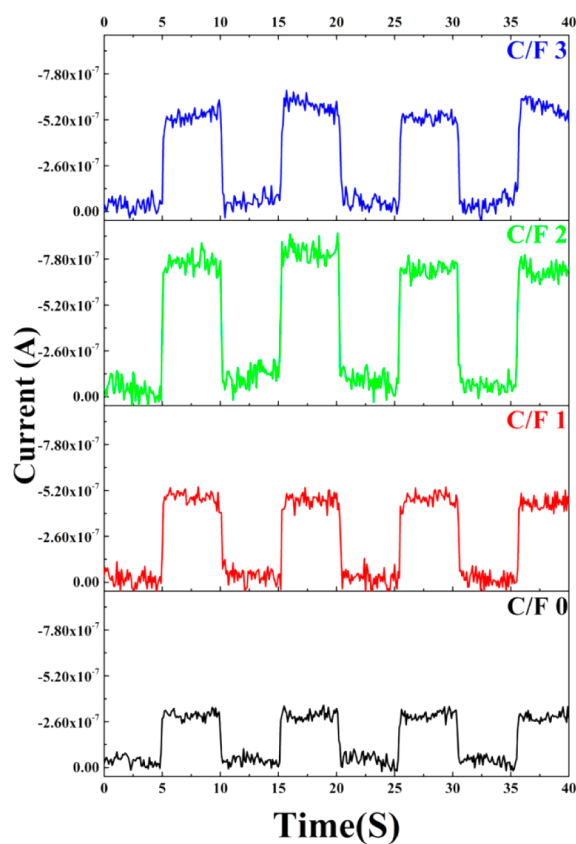


Figure 5. Photoelectric properties of C QDs/p-type  $\text{CuAlO}_2$ /n-type ZnO film composites with different amounts of C QDs.



temperature with illumination and darkness switching every 5 s without bias voltage. It is interesting that the samples exhibit high photosensitivity after C QDs were attached on the surface of the devices. As can be seen, the photosensitivity increases gradually with an increase in the concentration of C QDs from 0 to 2 mg/mL and then decreases to 3 mg/mL. When the photocurrents are  $2.98 \times 10^{-7}$ ,  $4.97 \times 10^{-7}$ ,  $7.83 \times 10^{-7}$ , and  $5.96 \times 10^{-7}$  A, respectively, the photoelectric properties are optimized at the compound concentration of 2 mg/mL, which indicates that introducing a suitable amount of C QDs can effectively improve the visible-light responsivity.

As is known, the essences of the photoelectric device are the illumination intensity and carrier concentration. Therefore, it is significant for us to investigate the role of C QDs in the composites.

In this C QDs/p-type CuAlO<sub>2</sub>/n-type ZnO device, the photoconductor is mainly from a photogenerated carrier (holes from CuAlO<sub>2</sub> and electrons from ZnO). So, the simplified formula for the conductivity could be fitted as  $\Delta\sigma = \Delta\delta\mu q$ ,<sup>21,25</sup> where  $q$  denotes the carrier charge,  $\Delta\delta$  denotes the change of the carrier concentration (holes for CuAlO<sub>2</sub> and electrons for ZnO), and  $\mu$  denotes the carrier mobility. From this formula, it can be inferred for wide-band-gap semiconductors that efficiently utilizing the luminous energy (especially  $\lambda_{\text{ZnO}} \leq 380$  and  $\lambda_{\text{CuAlO}_2} \leq 360$ ) to excite the photogenerated carrier is the most important way.

In sunlight, all of the components are certain, and most of them are visible light, so in our design, we expect to convert the visible light to shorter wavelengths. Compared with traditional semiconductor QDs, C QDs with its unique up-converted PL can absorb visible and near-infrared light and then convert them to shorter wavelengths,<sup>26–28</sup> which is one of the potential materials that we desire. Figure 6a shows the up-converted PL

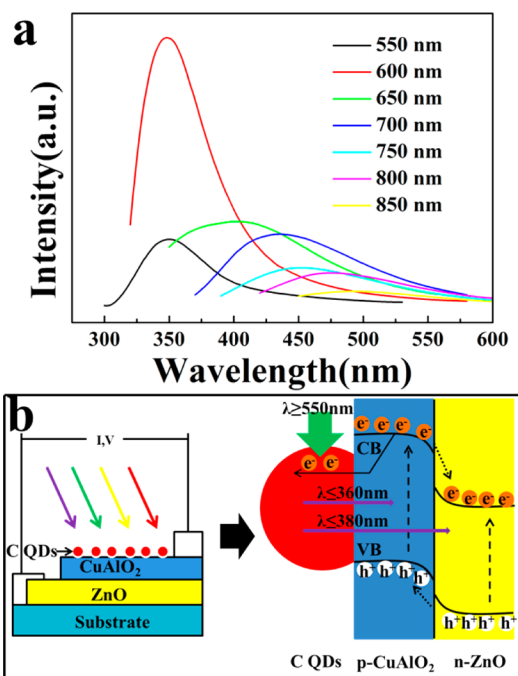


**Figure 6.** (a) Up-converted PL spectra of C QDs with excitation of visible–near-infrared wavelengths. (b) Schematic illustration for the photovoltaic process of C QDs/p-type CuAlO<sub>2</sub>/n-type ZnO film composites under irradiation.

spectra of C QDs measured using excitation wavelengths ranging from 550 to 850 nm. The curves indicate that the up-converted emission is located near 360 nm and exhibits an excitation-dependent behavior, which is corresponds with what was previously reported.<sup>29</sup> Figure 6b describes the schematic diagram. As is shown, after C QDs were introduced into the composite system, a part of the visible light was converted to shorter wavelength, which may increase the photogenerated electron–hole pairs to enhance the photoconductivity. In this C QDs/p-type CuAlO<sub>2</sub>/n-type ZnO device, the resistance of p-type CuAlO<sub>2</sub> is considered as the main factor (which is much greater than that of ZnO). The light ( $\lambda \leq 360$ ) could excite CuAlO<sub>2</sub> to increase photogenerated holes, and the extra electrons may drift to ZnO to promote the separation of photogenerated electron–hole pairs, which is one of the most important reasons for the conductivity. What is more, as shown in Figure 6b, C QDs can accept the photogenerated electrons from the semiconductor to promote the separation also. Similar results were reported by Liu et al. and Pu et al.<sup>18,30</sup> This is another important reason for increasing the carrier concentration, while it is interesting that an excess amount of C QDs leads to a slight decrease of the photocurrent. As is known, C QDs can absorb most of the light in spite of lacking excellent conductivity,<sup>18</sup> and limited by the quantum yield, a higher content of C QDs covered on the surface of film can result in a competition for light absorption, which may lead to decreasing photocurrent. In addition, extra C QDs may bring about a decrease in the transmittance, which is a disadvantage for application in windows. Because ZnO has a band gap that is narrower than CuAlO<sub>2</sub>, there is still a large amount of light with wavelength shorter than 380 nm that could irradiate through the upper film onto it, which can also increase the photocarriers and increase the photocurrent. From that above, the more efficiently utilized luminous energy and increasing carriers can promote enhancement of the photocurrent.<sup>21</sup> Compared with the p-type CuAlO<sub>2</sub>/n-type ZnO device, the photocurrent of the C QDs/p-type CuAlO<sub>2</sub>/n-type ZnO device can reach 260%.

On the other hand, the response time is another important property in the field of photoelectric detection device application. In this experiment, the photoresistance mainly depends on the resistance of CuAlO<sub>2</sub>, so the rising and decreasing times may be close to that of CuAlO<sub>2</sub>, which thus could be fitted by time as the formula  $\Delta\sigma = \beta\alpha I\tau(1 - e^{-t/\tau})$ , where  $\tau$  denotes the carrier life. So, the photoconductivity described by time could be shown as  $\Delta\sigma = \Delta\sigma_s(1 - e^{-t/\tau})$  and  $\Delta\sigma = \Delta\sigma_s e^{-t/\tau}$  when the photoconductivity decay to  $e^{-1}$  and enhance to  $1 - e^{-1}$ , respectively, where  $t$  is deemed as the response time.<sup>21</sup> By fitting the data, the rise and decay times of the C QDs/p-type CuAlO<sub>2</sub>/n-type ZnO composites are 130 and 115 ms, respectively. As can be seen, the quick-response time is one of the significant advantages for these devices to be applied in photovoltaic conversion.

#### 4. CONCLUSION

We have successfully prepared C QDs/p-type CuAlO<sub>2</sub>/n-type ZnO photoelectric bilayer film composites through a simple process and proved its excellent optical and photovoltaic conversion properties, which could be mainly attributed to the unique up-converted PL behavior of C QDs. In addition, the p–n junction structure and C QDs with the ability to accept electrons can help to separate the photogenerated electron–hole pairs for increasing the carrier concentration further. Under overall consideration, including the transmittance and

photosensitivity, the C/F 2 sample is demonstrated to be the preferable choice. Such novel photoelectric bilayer film composites may bring new insight to the design of transparent devices and promote potential photovoltaic conversion applications.

## ■ ASSOCIATED CONTENT

### ● Supporting Information

Structure and particle size distribution of the C QDs. This material is available free of charge via the Internet at <http://pubs.acs.org>.

## ■ AUTHOR INFORMATION

### Corresponding Authors

\*E-mail: [zhangxin@lzu.edu.cn](mailto:zhangxin@lzu.edu.cn).

\*E-mail: [fengbx@lzu.edu.cn](mailto:fengbx@lzu.edu.cn).

### Notes

The authors declare no competing financial interest.

## ■ ACKNOWLEDGMENTS

The authors gratefully acknowledge support for this work from the National Science Foundation of China (Grants 61176005 and 61006001) and Engagement Program (Program 2014046) funded by Xi'an University of Science and Technology.

## ■ REFERENCES

- (1) Wang, H.; Xiao, X. D.; Chen, T. Perovskite Photovoltaics: A High-Efficiency Newcomer to the Solar Cell Family. *Nanoscale* **2014**, *6*, 12287–12297.
- (2) Yun, S. N.; Hagfeldt, A.; Ma, T. L. Pt-Free Counter Electrode for Dye-Sensitized Solar Cells with High Efficiency. *Adv. Mater.* **2014**, *26*, 6210–6237.
- (3) Lee, D. C.; Brownell, L. V.; Yan, L.; You, W. Morphological Effects on the Small-Molecule-Based Solution-Processed Organic Solar Cells. *ACS Appl. Mater. Interfaces* **2014**, *6*, 15767–15773.
- (4) Pietruszka, R.; Luka, G.; Kopalko, K.; Zielony, E.; Bieganski, P.; Placzek-Popko, E.; Godlewski, M. Photovoltaic and Photoelectrical Response of n-ZnO/p-Si Heterostructures with ZnO Films Grown by an Atomic Layer Deposition Method. *Mater. Sci. Semicond. Process* **2014**, *25*, 190–196.
- (5) Lee, S. W.; Lee, Y. S.; Heo, J.; Siah, S. C.; Chua, D.; Brandt, R. E.; Kim, S. B.; Mailoa, J. P.; Buonassisi, T.; Gordon, R. G. Improved Cu<sub>2</sub>O-Based Solar Cells Using Atomic Layer Deposition to Control the Cu Oxidation State at the p-n Junction. *Adv. Energy Mater.* **2014**, *4*, 1301916.
- (6) Zhang, M.; Xu, K.; Jiang, X. S.; Yang, L.; He, G.; Song, X. P.; Sun, Z. Q.; Lv, J. G. Effect of Methanol Ratio in Mixed Solvents on Optical Properties and Wettability of ZnO Films by Cathodic Electrodeposition. *J. Alloys Compd.* **2014**, *615*, 327–332.
- (7) Tambasov, I. A.; Maygkov, V. G.; Tarasov, A. S.; Ivanenko, A. A.; Bykova, L. E.; Nemtsev, I. V.; Eremin, E. V.; Yozhikova, E. V. Reversible UV Induced Metal-Semiconductor Transition in In<sub>2</sub>O<sub>3</sub> Thin Films Prepared by Autowave Oxidation. *Semicond. Sci. Technol.* **2014**, *29*, 082001.
- (8) Goh, E. S. M.; Yang, H. Y.; Han, Z. J.; Chen, T. P.; Ostrikov, K. Controlled Electroluminescence of n-ZnMgO/p-GaN Light-emitting Diodes. *Appl. Phys. Lett.* **2012**, *101*, 263506.
- (9) Kawazoe, H.; Yasukawa, M.; Hyodo, H.; Kurita, M.; Yanagi, H.; Hosono, H. P-type Electrical Conduction in Transparent Thin Films of CuAlO<sub>2</sub>. *Nature* **1997**, *389*, 939–942.
- (10) Pan, J. Q.; Lan, W.; Liu, H. Q.; Sheng, Y. Z.; Feng, B. X.; Zhang, X.; Xie, E. Q. Preparation and Properties of Transparent Conductive N-Doped CuAlO<sub>2</sub> Films Using N<sub>2</sub>O as the N Source. *J. Mater. Sci.: Mater. Electron.* **2014**, *25*, 4004–4007.

- (11) Smith, J. R.; Van Steenkiste, T. H.; Wang, X. G. Thermal Photocatalytic Generation of H<sub>2</sub> over CuAlO<sub>2</sub> Nanoparticle Catalysts in H<sub>2</sub>O. *Phys. Rev. B: Condens. Matter Mater. Phys.* **2009**, *79*, 041403.
- (12) Wongcharoen, N.; Gaewdang, T. Thermoelectric Properties of Ni-Doped CuAlO<sub>2</sub>. *Phys. Procedia* **2009**, *2*, 101–106.
- (13) Kim, D. S.; Park, T. J.; Kim, D. H.; Choi, S. Y. Fabrication of a Transparent p–n Heterojunction Thin Film Diode Composed of p-CuAlO<sub>2</sub>/n-ZnO. *Phys. Status Solidi A* **2006**, *203*, R51–R53.
- (14) Banerjee, A. N.; Nandy, S.; Ghosh, C. K.; Chattopadhyay, K. K. Fabrication and Characterization of All-Oxide Heterojunction p-CuAlO<sub>2+x</sub>/n-Zn<sub>1-x</sub>Al<sub>x</sub>O Transparent Diode for Potential Application in “Invisible Electronics”. *Thin Solid Films* **2007**, *515*, 7324–7330.
- (15) Briscoe, J.; Marinovic, A.; Sevilla, M.; Dunn, S.; Titirici, M. Biomass-Derived Carbon Quantum Dot Sensitizers for Solid-State Nanostructured Solar Cells. *Angew. Chem., Int. Ed.* **2015**, *54*, 4463–4468.
- (16) Zhang, N.; Zhang, Y. H.; Xu, Y. J. Recent Progress on Graphene-Based Photocatalysts: Current Status and Future Perspectives. *Nanoscale* **2012**, *4*, 5792–5813.
- (17) Wei, J. M.; Zhang, X.; Sheng, Y. Z.; Shen, J. M.; Huang, P.; Guo, S. K.; Pan, J. Q.; Feng, B. X. Dual Functional Carbon Dots Derived from Cornflour via a Simple One-Pot Hydrothermal Route. *Mater. Lett.* **2014**, *123*, 107–111.
- (18) Yu, X. J.; Liu, J. J.; Yu, Y. C.; Zuo, S. L.; Li, B. S. Preparation and Visible Light Photocatalytic Activity of Carbon Quantum dots/TiO<sub>2</sub> Nanosheet Composites. *Carbon* **2014**, *68*, 718–724.
- (19) Xie, C.; Nie, B.; Zeng, L. H.; Liang, F. X.; Wang, M. Z.; Luo, L. B.; Feng, M.; Yu, Y. Q.; Wu, C. Y.; Wu, Y. C.; Yu, S. H. Core–Shell Heterojunction of Silicon Nanowire Arrays and Carbon Quantum Dots for Photovoltaic Devices and Self-Driven Photodetectors. *ACS Nano* **2014**, *8*, 4015–4022.
- (20) Zhang, Y. H.; Tang, Z. R.; Fu, X. Z.; Xu, Y. J. TiO<sub>2</sub>–Graphene Nanocomposites for Gas-Phase Photocatalytic Degradation of Volatile Aromatic Pollutant: Is TiO<sub>2</sub>–Graphene Truly Different from Other TiO<sub>2</sub>–Carbon Composite Materials? *ACS Nano* **2010**, *4*, 7303–7314.
- (21) Pan, J. P.; Guo, S. K.; Zhang, X.; Feng, B. X.; Lan, W. The Photoconductivity Properties of Transparent Ni Doped CuAlO<sub>2</sub> Films. *Mater. Lett.* **2013**, *96*, 31–33.
- (22) Li, Y.; Zhang, B. P.; Zhao, J. X.; Ge, Z. H.; Zhao, X. K.; Zou, L. ZnO/Carbon Quantum Dots Heterostructure with Enhanced Photocatalytic Properties. *Appl. Surf. Sci.* **2013**, *279*, 367–373.
- (23) Li, X. H.; Niu, J. L.; Zhang, J.; Li, H. L.; Liu, Z. F. Labeling the Defects of Single-Walled Carbon Nanotubes Using Titanium Dioxide Nanoparticles. *J. Phys. Chem. B* **2003**, *107*, 2453–2458.
- (24) Bu, I. Y. Y. Optoelectronic Properties of Novel Amorphous CuAlO<sub>2</sub>/ZnO NWs Based Heterojunction. *Superlattices Microstruct.* **2013**, *60*, 160–198.
- (25) Porat, O.; Riess, I. Defect Chemistry of Cu<sub>2-x</sub>O at Elevated Temperatures. Part II: Electrical Conductivity, Thermoelectric Power and Charged Point Defects. *Solid State Ionics* **1995**, *81*, 29–41.
- (26) Liang, Q. H.; Ma, W. J.; Shi, Y.; Li, Z.; Yang, X. M. Easy Synthesis of Highly Fluorescent Carbon Quantum Dots from Gelatin and Their Luminescent Properties and Applications. *Carbon* **2013**, *60*, 421–428.
- (27) Li, H. T.; Liu, R. H.; Liu, Y.; Huang, H.; Yu, H.; Ming, H.; Lian, S. Y.; Lee, S. T.; Kang, Z. H. Carbon Quantum Dots/Cu<sub>2</sub>O Composites with Protruding Nanostructures and Their Highly Efficient (Near) Infrared Photocatalytic Behavior. *J. Mater. Chem.* **2012**, *22*, 17470–17475.
- (28) Zhang, H. C.; Huang, H.; Ming, H.; Li, H. T.; Zhang, L. L.; Liu, Y.; Kang, Z. H. Carbon Quantum Dots/Ag<sub>3</sub>PO<sub>4</sub> Complex Photocatalysts with Enhanced Photocatalytic Activity and Stability under Visible Light. *J. Mater. Chem.* **2012**, *22*, 10501–10506.
- (29) Pan, J. Q.; Sheng, Y. Z.; Zhang, J. X.; Wei, J. M.; Huang, P.; Zhang, X.; Feng, B. X. Preparation of Carbon Quantum Dots/TiO<sub>2</sub> Nanotubes Composites and Their Visible Light Catalytic Applications. *J. Mater. Chem. A* **2014**, *2*, 18082–18086.
- (30) Pu, X. P.; Zhang, D. F.; Gao, Y. Y.; Shao, X.; Ding, G. Q.; Li, S. S.; Zhao, S. P. One-Pot Microwave-Assisted Combustion Synthesis of

Graphene Oxide–TiO<sub>2</sub> Hybrids for Photodegradation of Methyl Orange. *J. Alloys Compd.* **2013**, *551*, 382–388.